

benzene is added. We are hesitant to attach significance to this, because it is barely greater than the experimental precision. However, other investigators have noticed a similar phenomenon at infinite dilution using gc¹² or at very low solvent fraction using a McBain balance.¹³ The value of

(12) R. D. Newman and J. M. Prausnitz, paper presented at the 64th Annual Meeting of the American Institute of Chemical Engineers, San Francisco, Calif., Dec 1, 1971.

(13) D. Bonner and J. M. Prausnitz, personal communication.

0.325 is consistent with what is normal for a nonpolar system at these conditions.

Finally, the parameters following for each system were used in eq 6 to compute the *K* curves shown in Figure 1: benzene-polystyrene, $r = 0.768$, $\chi = 0.325$; *n*-decane-high-density polyethylene, $r = 0.785$, $\chi = 0.12$. The utility of correlating these amorphous systems by eq 6 is apparent.

Acknowledgments. The authors thank Amoco Chemicals Corporation for permission to publish these results.

Molecular Weight Distribution of Synthetic Stereoregular Polysaccharides. I. Method of Sedimentation Velocity

J.-P. Merle and A. Sarko*

Department of Chemistry, State University College of Forestry, Syracuse, New York 13210.
Received October 15, 1971

ABSTRACT: The applicability of the sedimentation velocity method for the determination of molecular weight distributions of synthetic, stereoregular tribenzyl glucans was investigated. Moderate to severe dependencies on pressure and concentrations, accompanied by diffusion, were observed with two polymers of low to medium polydispersity. The corrections for these effects were applied in a sequential manner, treating each effect independently from others. Polydispersities obtained from the corrected sedimentation coefficient distributions compared favorably with polydispersities obtained by independent methods.

The synthesis of stereoregular linear α -1,6-linked polysaccharides is under detailed investigation at this laboratory.¹⁻¹⁰ These studies have created a need for a relatively rapid and reliable method for the characterization of molecular weight distributions of the polymers. The requirements of the method include applicability to both the water-soluble parent polysaccharides and their derivatives soluble only in organic solvents, to molecular weight distributions of both narrow as well as moderate polydispersity, and to solutions not at their Θ temperature. Of a number of possible experimental techniques available for this purpose, the method of sedimentation velocity was investigated first. The latter technique has been used in the characterization of a number of synthetic polymers with apparent success, especially with polymers of narrow polydispersity and under Θ conditions.¹¹⁻¹⁶ In addition, the theory of sedimentation velocity is well understood.¹⁷

In the following, we report on the application of the sedi-

mentation velocity method to two different high molecular weight tribenzyl derivatives of α -1,6-glucan, one of relatively narrow and the other of moderate polydispersity.

Theory

A system which is heterogeneous with respect to mass yields under the conditions of a sedimentation transport experiment a distribution of sedimentation coefficients. The sedimentation coefficient, *S*, which is defined

$$S = (dr/dt)(1/\omega^2 r) \quad (1)$$

is related to the mass of the molecule, *m*, by

$$S = m(1 - \bar{v}\rho)/f \quad (2)$$

where *r* is the distance from the center of revolution to a specified point in the ultracentrifuge cell, *t* is the time from the start of sedimentation, ω is the angular velocity of revolution, \bar{v} is the partial specific volume of the molecule, *f* is its frictional coefficient, and ρ is the density of the solvent.

In general, for a polydisperse material, we can write that the fraction of material with sedimentation coefficient between *S* and *S* + *dS* is *g(S)dS*. If for the present we neglect the effects of concentration, diffusion, and pressure, it is easily shown that the distribution of material with different *S* in a sector-shaped ultracentrifuge cell is given by

$$g(S) = \frac{1}{c_0} \frac{dc_0}{dS} = \frac{1}{c_0} \left(\frac{dc}{dr} \right) \left(\frac{r}{r_0} \right)^2 r \omega^2 t \quad (3)$$

where *c* is concentration, *c*₀ is the initial concentration, and *r*₀ is the position of the meniscus.¹⁸ When Schlieren optics are

- (1) C. C. Tu and C. Schuerch, *J. Polym. Sci., Part B*, **1**, 163 (1963).
- (2) E. R. Ruckel and C. Schuerch, *J. Org. Chem.*, **31**, 2233 (1966).
- (3) J. Zachoval and C. Schuerch, *J. Amer. Chem. Soc.*, **91**, 1165 (1969).
- (4) J. Frechet and C. Schuerch, *ibid.*, **91**, 1161 (1969).
- (5) T. Uryu, H. Libert, J. Zachoval, and C. Schuerch, *Macromolecules*, **3**, 345 (1970).
- (6) E. R. Ruckel and C. Schuerch, *J. Amer. Chem. Soc.*, **88**, 2605 (1966).
- (7) E. R. Ruckel and C. Schuerch, *Biopolymers*, **5**, 515 (1967).
- (8) B. Veruovic and C. Schuerch, *Carbohydr. Res.*, **14**, 199 (1970).
- (9) V. Masura and C. Schuerch, *ibid.*, **15**, 65 (1970).
- (10) T. Uryu and C. Schuerch, *Macromolecules*, **4**, 342 (1971).
- (11) M. Wales and S. J. Rehfeld, *J. Polym. Sci.*, **62**, 179 (1962).
- (12) I. H. Billick, *ibid.*, **62**, 167 (1962).
- (13) J. E. Blair and J. W. Williams, *J. Phys. Chem.*, **68**, 161 (1964).
- (14) A. F. V. Eriksson, *Acta Chem. Scand.*, **10**, 360 (1956).
- (15) H. W. McCormick, *J. Polym. Sci., Part A*, **1**, 103 (1963).
- (16) H.-J. Cantow, *Makromol. Chem.*, **30**, 169 (1959).
- (17) H. Fujita, "Mathematical Theory of Sedimentation Analyses," Academic Press, New York, N. Y., 1962.
- (18) H. K. Schachman, "Ultracentrifugation in Biochemistry," Academic Press, New York, N. Y., 1959, Chapter IV.

used, the above equation is given more commonly in terms of the experimentally obtainable quantity dn/dr

$$g(S) = \frac{1}{n_0} \left(\frac{dn}{dr} \right) \left(\frac{r}{r_0} \right)^2 r \omega^2 t \quad (4)$$

where n_0 is the refractive index difference between the starting solution and the solvent and the refractive index gradient dn/dr is assumed to be given by

$$dn/dr = (dc/dr)(dn/dc) \quad (5)$$

In reality, the effects of concentration, diffusion, and pressure cannot be ignored, especially when one deals with a low molecular weight polymer dissolved in a relatively compressible organic solvent which also happens to be a good solvent for the polymer.^{17,18} The concentration dependence of the sedimentation coefficient is empirically expressed either by

$$S = S_0(1 - kc) \quad (6)$$

or by

$$1/S = (1/S_0)(1 + k'c) \quad (7)$$

where S_0 is the value of S at infinite dilution and k and k' are constants.¹⁸ Fujita has shown that for a monodisperse system in which diffusion is negligible, both concentration and pressure effects can be simultaneously treated in terms of eq 7 and a single pressure dependent parameter, m

$$m = (1/2)\mu\omega^2 r_0^2 \rho \quad (8)$$

where μ is a constant characteristic of the solute-solvent system.¹⁷ For a polydisperse system, a similar solution is not available. However, it has been shown that the concentration and pressure dependencies of the sedimentation coefficient may be treated separately, the former in terms of eq 6 or 7 and the latter in terms of the same pressure-dependent parameter m (eq 8).¹² The pressure-corrected sedimentation coefficient, S^0 , at a given concentration is given by¹²

$$S = S^0[1 - m_a(\gamma - 1)] \quad (9)$$

where m_a is the pressure-dependent parameter applicable to that concentration and $\gamma = (r/r_0)^2$. The value of S^0 is then corrected to infinite dilution according to eq 6 or 7.

Similarly, it has been shown that diffusion effects may be removed separately by extrapolation of S to infinite time.¹⁸

In practice, then, the observed distribution of sedimentation coefficients (denoted by $g^*(S)$) in a polydisperse system subject to concentration, pressure, and diffusion effects may be corrected for all three effects sequentially, starting with pressure and ending with concentration.

The resulting distribution of sedimentation coefficients, $g(S_0)$, at atmospheric pressure, in the absence of diffusion and at infinite dilution, may be related to molecular weight distribution in the following fashion.¹¹ The sedimentation constant S_0 , the molecular weight M , and the intrinsic viscosity $[\eta]$ are related by

$$M = [S_0 \eta_0 N / (1 - \bar{v} \rho) \beta]^{3/2} [\eta]^{1/2} \quad (10)$$

and

$$[\eta] = KM^a \quad (11)$$

where η_0 is the solvent viscosity, N is Avogadro's number, and $\beta = \Phi^{1/3} P^{-1}$ as defined by Flory.¹⁹ In terms of $f(M)$,

(19) P. J. Flory, "Principles of Polymer Chemistry," Cornell University Press, Ithaca, N. Y., 1953, Chapter XIV.

TABLE I
SAMPLE CHARACTERISTICS

Code no.	\bar{M}_w (light scattering)	\bar{M}_n (osmometry)	\bar{M}_w/\bar{M}_n	$[\eta]^{25^\circ \text{benzene}}$	\bar{v}
LGB-38	1.86×10^5	1.29×10^5	1.4	0.086	0.74
GL-21	8.89×10^5	3.47×10^5	2.5	0.225	0.74

the weight-differential distribution function, one can immediately write

$$[\eta] = K \int_0^\infty M^a f(M) dM = K \int_0^\infty M^a g(S_0) dS_0 \quad (12)$$

where K and a are the constants in the intrinsic viscosity-molecular weight relationship (eq 11).¹¹ Following Wales and Rehfeld, we can define a sedimentation-velocity-average molecular weight

$$M_{sv} = \left[\frac{\eta_0 N}{(1 - \bar{v} \rho) \beta} \right]^{3/2} [\eta]^{1/2} S_{0\max}^{3/2} \quad (13)$$

where $S_{0\max}$ is the sedimentation constant of the maximum in the $g(S_0)$ distribution.¹¹ Now, the $f(M)$ distribution as well as both weight- and number-average molecular weights are easily derived.¹¹

$$f(M) = \frac{2 - a}{3} \frac{g(S_0)_0}{M_{sv}} \frac{S_{0\max}^{3/2}}{S_0^{1+a/2-a}} \left[\int_0^\infty S_0^{3a/2-a} g(S_0) dS_0 \right]^{1/2} \quad (14)$$

$$M = \frac{S_0^{3/2-a} M_{sv}}{S_{0\max}^{3/2} \left[\int_0^\infty S_0^{3a/2-a} g(S_0) dS_0 \right]^{1/2}} \quad (15)$$

$$\bar{M}_w = \int_0^\infty M f(M) dM = \frac{M_{sv}}{S_{0\max}^{3/2}} \frac{\int_0^\infty S_0^{3/2-a} g(S_0) dS_0}{\left[\int_0^\infty S_0^{3a/2-a} g(S_0) dS_0 \right]^{1/2}} \quad (16)$$

$$\bar{M}_n = \frac{1}{\int_0^\infty \frac{1}{M} f(M) dM} = \frac{M_{sv}}{S_{0\max}^{3/2}} \times \frac{1}{\int_0^\infty S_0^{-3/2-a} g(S_0) dS_0 \left[\int_0^\infty S_0^{3a/2-a} g(S_0) dS_0 \right]^{1/2}} \quad (17)$$

From relations 16 and 17, the polydispersity index \bar{M}_w/\bar{M}_n is given simply by

$$\frac{\bar{M}_w}{\bar{M}_n} = \int_0^\infty S_0^{3/2-a} g(S_0) dS_0 \int_0^\infty S_0^{-3/2-a} g(S_0) dS_0 \quad (18)$$

a relation which involves no molecular parameters.¹¹

Experimental Section

Samples. The two benzylated linear α -1,6-glucans used in this work were previously synthesized.¹¹ The sample codes and their molecular weights are given in Table I. Similar polymers had been previously shown to be 97–99% stereoregular.

Sedimentation Experiments. All sedimentation measurements were made at 8° in a Spinco Model E analytical ultracentrifuge equipped with an An-D rotor, temperature control, and Schlieren

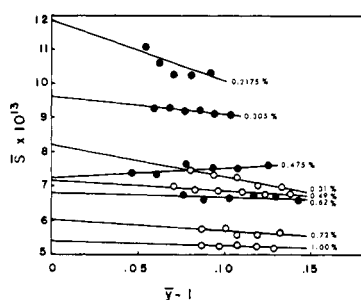


Figure 1. Plots of $\ln \bar{y}/2\omega^2 t$ vs. $\bar{y} - 1$ for different concentrations: (O) sample LGB-38, (●) sample GL-21.

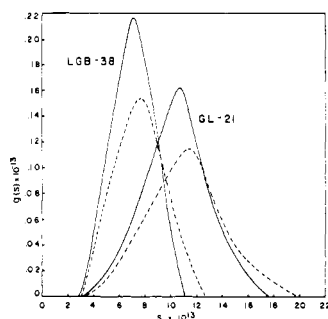


Figure 2. Effect of pressure correction on distribution of sedimentation coefficients: (—) uncorrected, (---) corrected; sample LGB-38 $c = 0.31\%$, $t = 4600$ sec; sample GL-21 $c = 0.2175\%$, $t = 2200$ sec.

optics. A double-section 12-cm cell with an aluminum-filled centerpiece and plain quartz windows was used. The polymer was dissolved in benzene (Fischer, spectral grade), and typical solution concentrations were 2–10 mg/ml. The centrifuge was operated at a speed of 42,040 rpm in all cases. Acceleration was held constant until the final speed was reached and $t = 0$ was taken at the time of two-thirds of the final speed. The boundary gradient curves were recorded photographically at intervals of 4 or 8 min. The photographic curves were traced on graph paper at approximately $5\times$ magnification with the help of a photographic enlarger. All subsequent measurements were performed on the enlarged tracings.

In order to achieve maximum recording sensitivity, the Schlieren angle was varied with the concentration of the solution: the lower the concentration the lower was the angle to maximize the area under the boundary curve.

Calculations. The individual tracings of the boundary gradient curves were divided into increments along the abscissa (20–40 increments) and pairs of r and $(dn/dr)_{app}$ values were read for each increment. The pressure correction parameter m_a (cf. eq 9) was then obtained for each concentration by plotting $\ln \bar{y}/2\omega^2 t$ vs. $\bar{y} - 1$, where the average \bar{y} was computed for each time t from¹²

$$\bar{y} = \frac{\sum_i y_i (dn/dr)_i dr}{\sum_i (dn/dr)_i dr} \quad (19)$$

where the $(dn/dr)_i$'s are the values of $(dn/dr)_{app}$ corrected in the usual manner for Schlieren angle and instrumental constants (cf. Spinco Model E manual).

The pressure-corrected $g(S)$ vs. S distribution curve was obtained from¹²

$$g(S) = \frac{1}{A_0} \left(\frac{dn}{dr} \right)_{app} \left(\frac{r}{r_0} \right)^2 r \omega^2 t [1 - m_a(y - 1)]^2 \quad (20)$$

and

$$S = \frac{1}{2(m_a + 1)\omega^2 t} \ln \frac{y}{1 - m_a(y - 1)} \quad (21)$$

where A_0 is the total area under the boundary gradient curve.

The individual $g(S)$ vs. S distribution curves for each time t (for a given concentration) were then extrapolated to infinite time by plotting values of $g(S)$ at constant S vs. $1/t$. The resulting single distribution curve for each concentration, $g(S^0)$ vs. S^0 , now corrected for both pressure and diffusion, was then normalized to unit area to correct for extrapolative errors.

Finally, the individual $g(S^0)$ vs. S^0 distributions were extrapolated to infinite dilution in two ways: (1) by plotting S^0 vs. c at constant $g(S^0)/g_{max}(S^0)$, and (2) by plotting $1/S^0$ vs. c in the same manner.²⁰ This procedure resulted in the final distribution curve $g(S_0)$ vs. S_0 , which is corrected to atmospheric pressure, absence of diffusion, and infinite dilution.

The actual calculations were performed with a plotter-equipped IBM 1620-II computer and a program specially developed for this purpose.²¹

Results and Discussion

Pressure Correction. The plots of $\ln \bar{y}/2\omega^2 t$ vs. $\bar{y} - 1$ from which the pressure-correction parameters m_a were calculated are shown in Figure 1 for all concentrations of the two polymers used in this experiment. In general, the plots are linear, with pronounced slopes at low concentrations which decrease markedly as the concentration increases. It is also evident that considerable scatter is present in some of the plots, which results in one case (0.475%) in a positive slope, indicating the impossible situation of decreasing pressure with increasing distance from the center of rotation. The scatter in the data stems to a large extent from the fact that a precision plate reading microscope was not available.

The increasing negative slope in the plots with decreasing concentration simply points out that the pressure-correction parameter is not independent of concentration. A similar tendency appears to occur in studies with polystyrene.¹²

The effects of pressure correction are shown in Figure 2 for the two lowest concentrations of both polymer samples. The pressure-correction parameters for these concentrations at values of $m_a = 1.57$ for GL-21 and $m_a = 1.14$ for LGB-38 were the largest of all concentrations. The uncorrected distribution curves were calculated from eq 4 for $g^*(S)$ and from $S = \ln y/2\omega^2 t$, while the pressure-corrected distribution curves were obtained from eq 20 and 21. It is clear that the pressure effect even at the relatively low velocity of 42,040 rpm is considerable, causing a significant skewing of the distribution toward lower values of the sedimentation coefficient. This causes a significant sharpening of the distribution which could be especially troublesome when polydispersity is large. It is interesting to note that the pressure effects in both samples are comparable, indicating no significant superimposed effects of polydispersity or molecular weight within the range covered by the two samples.

The pressure effects at higher concentrations are proportionately less, but never become insignificant and thus cannot be neglected.

Diffusion Correction. The correction for diffusion effects was accomplished, as previously explained, by plotting the pressure-corrected distributions against $1/t$ and extrapolating to $1/t = 0$. The data, although somewhat scattered, fell on straight lines and presented no problems in extrapolating to infinite time. The scatter is again the consequence of im-

(20) R. L. Baldwin, *J. Amer. Chem. Soc.*, **76**, 402 (1954).

(21) A. Sarko and J.-P. Merle, to be published.

TABLE II
MOLECULAR WEIGHTS CALCULATED FROM THE DISTRIBUTION OF S_0

Sample	\bar{M}_w	\bar{M}_n	\bar{M}_w/\bar{M}_n
LGB-38	1.2×10^5	7.3×10^4	1.6
GL-21	6.5×10^5	2.8×10^5	2.3

precise reading of plates and is usually slightly worse for low concentrations at long sedimentation times.

The extrapolation indicates the presence of considerable diffusion which, when corrected for, results in appreciably sharper distributions. This effect is illustrated in Figure 3. The diffusion effects could probably be lessened by increasing the rotor velocity; however, this would aggravate pressure effects, thus resulting in, at best, questionable improvements.

The magnitude of diffusion was comparable in both samples, indicating again no marked influence of molecular weight or polydispersity.

Concentration Effects. The pressure- and diffusion-corrected distribution curves for all concentrations of the two polymers are shown in Figures 4 and 5. It is obvious that a concentration dependence is present to a marked degree in both cases. As previously indicated, the extrapolation to infinite dilution was attempted in two ways: one, by plotting S^0 against concentration, and the other by plotting $1/S^0$ in a similar manner. In both instances, reasonable linearity exists in most plots, although scatter becomes excessive near both tails of the distribution. This is again a consequence of poor precision in obtaining the data from the photographic plates.

Both resulting distributions at infinite dilution for sample LGB-38 are also shown in Figure 4. The distribution from $1/S^0$ vs. c is considerably broader than the corresponding curve from S^0 vs. c and is also shifted toward higher values of the sedimentation constant. As shown below, there is reason to believe that the distribution resulting from $1/S^0$ is the more correct one.

When the same extrapolations were attempted with the GL-21 sample, only the method of $1/S^0$ vs. c could be used because of systematic upward curvature in the S^0 vs. c plots at low concentrations and higher values of S^0 . In view of the higher degree of polydispersity and higher molecular weight of this polymer, the expected stronger concentration dependence would necessitate inclusion of other powers of c in the relation between S and c .²² The distribution at infinite dilution obtained from $1/S^0$ for this sample is shown in Figure 5 and can be seen to be quite broad.

Conversion to Molecular Weights. As shown in eq 14-18, the distribution of S_0 can be directly converted to distribution of M , provided the intrinsic viscosity, the Mark-Houwink exponent a , the Flory constant β , and the partial specific volume of the polymer are known. Knowing only the exponent a , one can still calculate the polydispersity ratio \bar{M}_w/\bar{M}_n .

Because the applicable value of the Flory constant β was not known in this instance, the complete molecular weight distribution curves were not calculated. However, using the known values of \bar{v} , $[\eta]$, and $a = 0.59$ for the two polymers, and assuming¹⁹ that $\beta = 2.5 \times 10^6$, values for \bar{M}_w , \bar{M}_n , and \bar{M}_w/\bar{M}_n were calculated from the distributions of S_0 derived from extrapolations of $1/S^0$ vs. c and are shown in Table II. Comparison with the experimentally determined values for the same parameters (cf. Table I) reveals a reasonably good correspondence for the polydispersity ratios, certainly within the

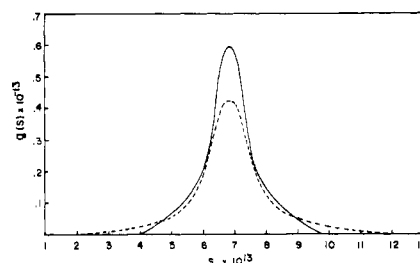


Figure 3. Effect of diffusion correction on the distribution of sedimentation coefficients: (—) corrected, (---) uncorrected; sample GL-21 $c = 0.62\%$, uncorrected $t = 2800$ sec.

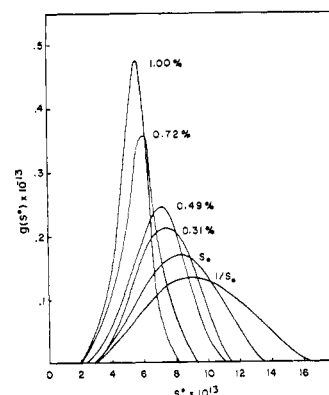


Figure 4. Pressure- and diffusion-corrected sedimentation coefficient distributions at different concentrations and distributions at infinite dilution for sample LGB-38. The curve marked S_0 was obtained by extrapolation of S^0 vs. c to $c = 0$, and the curve marked $1/S_0$ was obtained from similar extrapolation of $1/S^0$ vs. c .

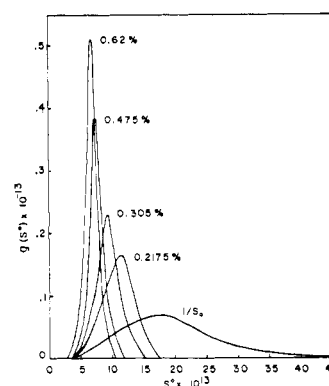


Figure 5. Same as in Figure 4, but for sample GL-21.

accepted experimental errors of the osmometric and light-scattering techniques. The calculated average molecular weights are, however, significantly lower. The comparison of calculated and experimental polydispersity ratios is the most valid of the three comparisons because the parameter β is not involved.

Similar calculations for the distribution curve for sample LGB-38 derived from extrapolation of the S^0 vs. c plots resulted in considerably smaller magnitudes for the three molecular weight parameters. For this reason, and because for sample GL-21 the S^0 vs. c plots were curved, it is believed that the distributions obtained from $1/S^0$ vs. c are the more correct of the two.

In conclusion, it is apparent that a further investigation of the application of the sedimentation velocity method is certainly warranted. Precision of experimental data recording seems especially critical and is most in need of improvement. The value for the parameter β must be obtained before meaningful conversion of the sedimentation constant distribution to molecular weight distribution can be accomplished. Finally, a comparison with a molecular weight

distribution obtained from an independent experimental technique is desirable.

Acknowledgment. This work has been supported by Research Grant No. GM 06168 from the Division of General Medical Science, National Institutes of Health. The authors are indebted to Mr. T. Bluhm for intrinsic viscosity, light-scattering, and partial specific volume measurements.

Effect of Pressure on the Second Virial Coefficient and Chain Dimensions in Polymer Solutions

D. Gaeckle and D. Patterson*

Chemistry Department, McGill University, Montreal, Canada. Received November 3, 1971

ABSTRACT: Second virial coefficients and radii of gyration at pressures up to 110 bars were determined at high polymer dilution for polyisobutylene in 2-methylbutane at 24, 57, and 64° and for polystyrene in 2-butanone at 22°, using SOFICA light-scattering equipment and a pressure-resistant cell. The results permit a calculation of the pressure dependence of the lower critical solution temperature of the polyisobutylene + 2-methylbutane system which is in good agreement with direct measurement. The pressure and temperature dependence of A_2 are consistent with newer theories of polymer solution thermodynamics. The dependences may be used to obtain relative partial molar volumes, $\Delta\bar{V}_1$, and heats, $\Delta\bar{H}_1$, of the solvent. Excluded-volume theories allow a comparison of $\Delta\bar{V}_1$ and $\Delta\bar{H}_1$ with literature values determined at high polymer concentration; agreement is fair. A correlation between values of $\langle S^2 \rangle^{1/2}$ and A_2 shows that pressure influences these quantities through its effect on the polymer-solvent interaction parameter χ or the z parameter.

Solution theories have traditionally emphasized an energetic contribution to the mixing functions arising from the relative weakness of contacts between molecules of different chemical nature and intermolecular force fields. Recent work^{1,2} in polymer solution thermodynamics shows the importance of a difference of free volumes, or degrees of thermal expansion, between the polymer and the solvent. During the mixing process, the free volumes move toward an intermediate value characteristic of the mixture. These changes produce major contributions (termed structural¹ or equation of state²) to the thermodynamic mixing functions, ΔH_M , ΔS_M , and ΔG_M as well as ΔV_M . The free volume contribution to ΔG_M and the interaction parameter, χ , is predicted to be positive. It accounts³ for the existence of the lower critical solution temperature occurring in polymer solutions at high temperature, where there is a large difference in free volume between polymer and solvent. The application of pressure will normally compress the solvent to a much greater extent than the polymer, thus reducing the free volume difference between them, and the corresponding contribution to ΔG_M and χ . Pressure does in fact markedly increase⁴ the value of the LCST, with a corresponding enhancement of polymer solubility. It is evident that pressure should have a large effect on quantities which reflect the polymer-solvent interaction, in particular the second virial coefficient, A_2 , and the radius of gyration of the macromolecule, $\langle S^2 \rangle^{1/2}$. Where the free volume contribution is dominant, i.e., at higher temperature or in systems where the disparity of intermolecular forces be-

tween the polymer and solvent is small, A_2 and $\langle S^2 \rangle^{1/2}$ should increase with pressure. This would correspond to a decrease of ΔG_M , or to a negative value of ΔV_M . At low temperature, however, approaching the upper critical solution temperature, the free volume contribution may be of less importance. Then the second virial coefficient and the polymer dimensions could decrease with pressure, corresponding to a positive value of ΔV_M .

Schulz and Lechner⁵⁻⁷ have pioneered in the study of the effect of pressure on light scattering in polymer solutions. Using a high-pressure optical cell and special instrumentation, they have made measurements up to 800 atm on a number of systems: polystyrene + *trans*-decalin, + toluene, + cyclohexane, and + chloroform. The results have been shown to be in qualitative and semiquantitative agreement with a theoretical treatment⁸ of pressure effects. In particular, $(\partial A_2 / \partial P)_T$ for polystyrene + *trans*-decalin^{5,6} is negative near the UCST ($\Theta = 19^\circ$) corresponding to $\Delta V_M > 0$. However, at higher temperature, $(\partial A_2 / \partial P)_T$ becomes positive (for small pressures), indicating that $\Delta V_M < 0$. The present work is an investigation of polyisobutylene (PIB) + 2-methylbutane and polystyrene (PS) + 2-butanone at lower pressure, using the standard SOFICA light-scattering equipment, and with new features of interpretation.

Thermodynamic Considerations

Relationship between the Pressure and Temperature Dependence of A_2 and the Partial Molar Volumes and Heats of the

(1) I. Prigogine (with the collaboration of V. Mathot and A. Belle-mans), "The Molecular Theory of Solutions," North Holland Publishing Co., Amsterdam, 1957.

(2) P. J. Flory, *Discuss. Faraday Soc.*, **No. 49**, 7 (1970).

(3) D. Patterson, *Macromolecules*, **2**, 672 (1969).

(4) (a) G. Allen and C. H. Baker, *Polymer*, **6**, 181 (1965); (b) L. Zeman, J. Biros, G. Delmas, and D. Patterson, *J. Phys. Chem.*, in press.

(5) G. V. Schulz and M. Lechner, *J. Polym. Sci., Part A-2*, **8**, 1885 (1970).

(6) M. Lechner and G. V. Schulz, *Eur. Polym. J.*, **6**, 945 (1970).

(7) G. V. Schulz and M. Lechner in "Light Scattering from Polymer Solutions," M. B. Huglin, Ed., Academic Press, New York, N.Y., 1971.

(8) D. Patterson and G. Delmas, *Trans. Faraday Soc.*, **65**, 708 (1969).